

Pulsed Nuclear Magnetic Resonance in Cesium Fluoride*

D. K. HUTCHINS† AND S. M. DAY

Department of Physics, University of Arkansas, Fayetteville, Arkansas 72701

(Received 21 November 1968)

Pulse nuclear-magnetic-resonance techniques have been used to obtain the free-induction-decay curves of both the F^{19} and Cs^{133} nuclear spin systems in single crystals of cesium fluoride. The experimental curves are compared with the theories of Gade and Lowe and of Lee, Tse, Goldberg, and Lowe. The F^{19} free induction decays can be satisfactorily described by considering only dipolar interactions among the nuclear spins. The Cs^{133} free induction decays are not in agreement with the predictions of dipolar theory. It is suggested that this departure is due to nuclear electric quadrupole effects.

INTRODUCTION

ONE of the fundamental problems in nuclear magnetic resonance (NMR) in solids is the calculation of the shape of the NMR absorption line, or equivalently, the free-induction-decay (fid) function. Gade and Lowe¹ (hereafter GL) have used an expansion technique first employed by Lowe and Norberg² to calculate the fid function in crystals having a single magnetic spin species for cases where there are dipolar and scalar exchange interactions.

More recently, Lee, Tse, Goldberg, and Lowe³ (hereafter LTGL) have extended this work to include spin systems containing two active magnetic ingredients of arbitrary spin which are coupled by dipolar and scalar exchange interactions. This theory was compared to experimental fid curves of Na^{23} resonance in NaCl where only dipolar coupling was considered in evaluating the theoretical expression.

In the work of LTGL, only one of the ingredients in the sample was studied. It therefore seemed desirable to subject the two-ingredient theory to an additional experimental test wherein the resonance of both species would be studied. The present paper presents the results of an experimental investigation by pulse NMR techniques of CsF single crystals. This material has NaCl-type crystal structure. The abundant isotopes are F^{19} and Cs^{133} with nuclear spin numbers $\frac{1}{2}$ and $\frac{7}{2}$, respectively.

In addition to the dipolar spin coupling, there is the possibility of quadrupole broadening of the Cs^{133} resonance due to the nonvanishing quadrupole moment of Cs^{133} nuclei (which has magnitude -3×10^{-27} cm²) interacting with electric field gradients due to defects in the crystal. Since Cs^{133} is a large atom, the electronic wave functions have a wide spatial extent, and a sizeable indirect exchange coupling of the nuclei via their electrons might be present. Whether or not these features play a significant role in determining the NMR line

shape can be decided by comparing the experimental fid curves with the predictions of dipolar theory.

Information about the line broadening mechanisms can also be gained by measurement of the "local field"⁴ at the nuclear sites, and by study of the cross-coupling transient (cct) using a technique described by Mansfield.⁵

THEORY

Generally, the Hamiltonian of a nuclear-spin system contained in an insulating solid includes interactions of the nuclear spins with the "lattice", dipolar couplings between pairs of nuclear spins, indirect scalar exchange interactions, nuclear-electric-quadrupole-moment-electric-field-gradient coupling, and the Zeeman energy of the nuclear spins in an externally applied magnetic field. The first of these can be ignored for discussion of a transient experiment if T_1 , the spin-lattice relaxation time, is long compared to the duration of the experiment.

When the sample is placed in a uniform static external field H_0 of several kG, the Zeeman term is generally much larger than the others, and the remaining terms can be treated as small perturbations on the Zeeman part. It is then a good approximation to drop nonsecular terms in the Hamiltonian, i.e., terms which do not conserve the Zeeman energy.

The Hamiltonian for a sample with two magnetic ingredients resulting from this truncation is

$$\mathcal{H} = \mathcal{H}_Z + \mathcal{H}_{SS} + \mathcal{H}_Q, \quad (1)$$

where

$$\begin{aligned} \mathcal{H}_Z &= -\hbar H_0 (\gamma_I \sum_i I_{zi} + \gamma_S \sum_{i'} S_{zi'}), \\ \mathcal{H}_{SS} &= \sum_{j < k} (A_{jk} \mathbf{I}_j \cdot \mathbf{I}_k + B_{jk} I_{zj} I_{zk}) \\ &\quad + \sum_{j' < k'} (A_{j'k'} \mathbf{S}_{j'} \cdot \mathbf{S}_{k'} + B_{j'k'} S_{zj'} S_{zk'}) \\ &\quad + \sum_{j < k'} A_{jk'} I_{zj} S_{zk'}, \\ \mathcal{H}_Q &= \sum_i K_i (3I_{zi}^2 - I_i^2). \end{aligned}$$

\mathcal{H}_Z is the Zeeman term, \mathcal{H}_{SS} represents spin-spin inter-

* Work supported by the National Science Foundation.
† Present address: Physics Department, State College of Arkansas, Conway, Ark.

¹ S. Gade and I. J. Lowe, Phys. Rev. **148**, 382 (1966).

² I. J. Lowe and R. E. Norberg, Phys. Rev. **107**, 46 (1957).

³ M. Lee, D. Tse, W. I. Goldberg, and I. J. Lowe, Phys. Rev. **158**, 246 (1967).

⁴ A. G. Redfield, Phys. Rev. **98**, 1787 (1955).

⁵ P. Mansfield, Phys. Rev. **137**, A961 (1965).

actions, and \mathcal{H}_Q is the quadrupolar Hamiltonian. In these expressions, \mathbf{I} and \mathbf{S} refer to the spin angular momentum operators of the resonant and nonresonant spins, respectively. Primed indices range over the nonresonant spins, and unprimed indices range over the resonant spins. Other symbols used are defined as follows:

$$A_{jk} = \tilde{A}_{jk} - \frac{1}{2}\gamma_j\gamma_k\hbar^2 r_{jk}^{-3}(1 - 3\cos^2\Theta_{jk}),$$

$$B_{jk} = \frac{3}{2}\gamma_j\gamma_k\hbar^2 r_{jk}^{-3}(1 - 3\cos^2\Theta_{jk}),$$

\tilde{A}_{jk} = coefficient of indirect scalar exchange coupling between nuclei j and k ,

γ_i = gyromagnetic ratio of spins of species i ,

$$K_i = [eQ/8I(2I-1)][(2\cos^2\Theta_E - 1)V_{ZZi} - \sin^2\Theta_E + \cos 2\Phi_E(V_{XXi} - V_{YYi})].$$

Here e is the proton charge and Q is the quadrupole moment of a resonant nucleus. The $V_{\alpha\alpha}$ are components of the symmetric tensor representing the electric field gradient as expressed in the principal axes system of the tensor. The angles Θ_E , Φ_E , Ψ_E are the Euler angles which take the principal axes of the tensor $V_{\alpha\beta}$ into the axes of the laboratory or Zeeman frame. Terms containing Ψ_E are nonsecular.

Following a 90° pulse which rotates the net magnetization vector of the resonant spins into the transverse plane, the evolution of the transverse component \mathfrak{M}_x of the net magnetization of the sample is given by

$$\langle \mathfrak{M}_x(t) \rangle = \text{Tr}\{e^{-(i/\hbar)\mathcal{H}t}\mathfrak{M}_x e^{(i/\hbar)\mathcal{H}t}\mathfrak{M}_x\} / \text{Tr}\{\mathfrak{M}_x^2\}, \quad (2)$$

where $\mathfrak{M}_x = \gamma_I \hbar I_x$, and $I_x = \sum_i I_{xi}$.

The envelope of this function is

$$F(t) = \text{Tr}\{e^{-(i/\hbar)\mathcal{H}t} I_x e^{(i/\hbar)\mathcal{H}t} I_x\} / \text{Tr}\{I_x^2\}, \quad (3)$$

and is called the fid. In this expression $\mathcal{H}_S = \mathcal{H}_{S^0} + \mathcal{H}_Q$. This function has been evaluated by GL for single ingredient systems with arbitrary spin in crystals where there are dipolar and scalar exchange interactions.

If a second 90° pulse of the same phase is applied to the sample at a time t after the first pulse, a signal resembling a solid echo generally results. Mansfield⁵ has shown that for two-ingredient systems with dipolar spin coupling this signal (called a cct) has the form

$$F(t') = [M_{2IS} t' \tau + M_{4IS1} (\tau^3 t' / 3!) + M_{4IS2} (\tau^2 t'^2 / 4!) + \dots], \quad (4)$$

where $t' = 0$ at $t = \tau$ and M_{2IS} is the second moment of the resonant spins due to their coupling with nonresonant spins. The M_{4ISi} are related to fourth moment contributions and include error terms.⁵

Taking the first time derivative and evaluating at $t' = 0$ yields

$$(d/dt)F(t')|_{t'=0} = [M_{2IS}\tau + M_{4IS1} - \tau^3/3! + \dots]. \quad (5)$$

For short t , it is expected that

$$M_{2IS} = (d/dt')F(t')|_{t'=0/\tau}. \quad (6)$$

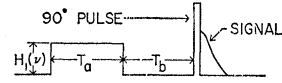


Fig. 1. Diagram of the pulse sequence used for the local-field measurements. Rise and fall times of the first pulse are about 4 μsec ; rise and fall times of the 90° pulse are 1 μsec .

A plot of initial cct slope against t would be linear and M_{2IS} could be measured.

A system of nuclear spins subjected to a radio-frequency (rf) field of saturating strength can be described in terms of a spin temperature in a frame rotating about H_0 at the frequency ν of the rf field. The rf field, of amplitude $2H_1$, is considered to be linearly polarized in a direction perpendicular to H_0 , the static external field. To be of saturating strength H_1 must satisfy the condition $\gamma_I^2 H_1^2 T_1 T_2 \gg 1$, where T_2 is of the order of the duration of the fid. This approach was proposed by Redfield⁴ and has been verified by experiment.⁶

Let such an rf field be applied at $t=0$ to a sample initially at thermal equilibrium with the lattice in \mathbf{H}_0 . For times t such that $T_2 \ll \tau \ll T_1$, this process can be described in the rotating frame as an isentropic demagnetization from a field \mathbf{H}_0 to a field $\mathbf{H}_{\text{eff}} = (H_0 + \nu/\tilde{\gamma})\hat{k} + H_1\hat{i}$, where $\tilde{\gamma} \equiv \gamma/2\pi$, so that $\nu/\tilde{\gamma} = \omega/\gamma$. The z component of the system magnetization, the component parallel to \mathbf{H}_0 , is given by⁶

$$\frac{M_z}{M_0} = \frac{(\Delta\nu)^2}{(\Delta\nu)^2 + \tilde{\gamma}_I^2 (H_1^2 + H_I^2)}. \quad (7)$$

Here M_0 is the thermal-equilibrium magnetization in the absence of H_1 , and $\Delta\nu = \nu - \nu_0$, where $\nu_0 = -\tilde{\gamma}_I H_0$. The quantity H_I called the local field, is defined by⁷

$$H_I^2 = \text{Tr}\{(\mathcal{H}_{S^0})^2\} / \text{Tr}\{\gamma_I^2 I_x^2\}. \quad (8)$$

In this expression, \mathcal{H}_{S^0} is the truncated spin Hamiltonian referred to the rotating frame and is identical to \mathcal{H}_S . Then $\mathcal{H}_{S^0}^2$ is given by⁷

$$\begin{aligned} H_I^2 = & \frac{1}{3} \langle \Delta H^2 \rangle_{II} + \langle \Delta H^2 \rangle_{IS} + \frac{1}{3} \frac{N_S (\gamma_S)^2 S(S+1)}{N_I (\gamma_I)} \frac{S(S+1)}{I(I+1)} \langle \Delta H^2 \rangle_{SS} \\ & + I(I+1) (N_I \hbar^2 \gamma_I^2)^{-1} \left[\sum_{j \neq k} \tilde{A}_{jk}^2 + \sum_{j' \neq k'} \tilde{A}_{j'k'}^2 \right] \\ & + \frac{3}{20} \frac{K_I}{\gamma_I^2} [4I(I+1) - 3], \quad (9) \end{aligned}$$

where N_i is the total number of spins of species i , and $\langle \Delta H^2 \rangle_{ij}$ is the contribution to the second moment of spins i due to spins j expressed in G.² In order to calculate the quadrupolar contribution to the local field,

⁶ W. I. Goldburg, Phys. Rev. **128**, 1554 (1962).

⁷ A complete discussion of H_I can be found in A. Abragam, *The Principles of Nuclear Magnetism* (Oxford University Press, New York, 1961).

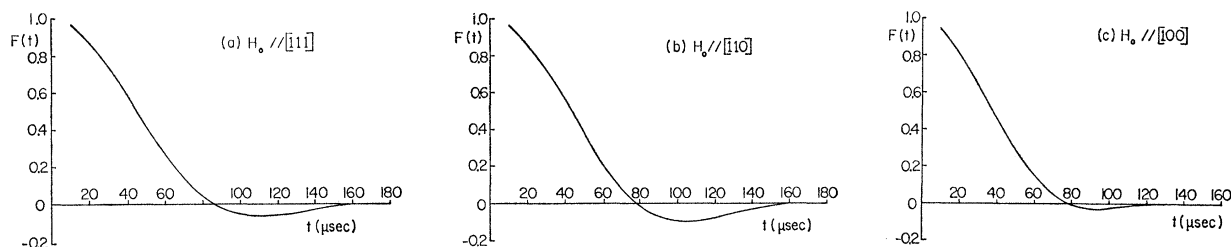


FIG. 2. Experimental free induction decays for the F^{19} nuclear-spin system in CsF.

it is necessary to know the distribution of electric field gradients at each nuclear site. As this distribution is not known, the K_i 's of Eq. (1) are assumed to all be equal, to obtain qualitative information.

EXPERIMENT

The measurements were made with a conventional coherent-pulse NMR apparatus employing a master oscillator and gated-power amplifier. The static field was produced by an electromagnet with 12-in. pole faces and $2\frac{1}{2}$ -in. gap. Static field inhomogeneity across the sample volume was determined to be less than 10 mG at a field strength of 5 kG by tests with proton resonance in water.

To obtain the fid curves the sample is first allowed to come into thermal equilibrium in the static field. Then the magnetization vector is rotated into the transverse plane by an rf pulse applied to the sample by means of a coil wound tightly on the thin-walled sample case. The resulting signal following the pulse is amplified and displayed directly on a calibrated oscilloscope where it can be photographed. In this apparatus a single coil is used both as a means of applying the pulses and as a pickup coil for the nuclear induction signal.

The F^{19} fid curves were obtained at a Larmor frequency of 20 MHz. The width of the 90° pulse was $3 \mu\text{sec}$. The Cs^{133} fid curves were observed at a Larmor frequency of 6 MHz and the 90° pulse width was $10 \mu\text{sec}$. Cross-coupling transients in both cases were found by applying a second 90° pulse of the same phase at a time $\tau \lesssim T_2$.

An experiment to measure the local field defined by Eq. (8) is performed by applying a pulse sequence as diagrammed in Fig. 1. The equipment is the same as employed in finding the fid curves, except that a second

transmitter is added to provide the first pulse of the sequence. The first pulse, of duration τ_a , frequency ν , and amplitude $2H_1$, is applied in the transverse plane and is of saturating strength. The time intervals τ_a and τ_b must satisfy the condition $T_2 \ll \tau_a, \tau_b \ll T_1$.

At the end of τ_b a 90° pulse of frequency $\nu_0 = \gamma_I H_0$ is applied. This gives rise to a free induction signal whose amplitude is proportional to the z magnetization at the end of τ_b . A plot of this amplitude as a function of $\Delta\nu = \nu - \nu_0$ can be compared directly to Eq. (7) to find H_L .

In the local field experiment, the value of H_1 must be known. This was found by increasing H_1 until a 90° pulse could be produced for proton resonance in a water sample placed in the sample cavity. A correspondence is established between the magnitude of H_1 and the peak to peak voltage at the transmitter terminals. Values of H_1 at a particular voltage are found by extrapolation of this linear function.

The quantity $\Delta\nu$ is the difference between the frequencies of the two signal generators supplying the cw rf for the pulses. This is measured by coupling the output of each to a short-wave receiver and viewing the beat frequency on a calibrated oscilloscope. In this way $\Delta\nu$ could be measured to ± 50 Hz.

In a two species sample, the resonance of spins I can be narrowed⁸ by rf stirring of the spins S . This is accomplished by subjecting the nonresonant spins S to a strong rf field at their resonant frequency. This tends to average out the local field "seen" by spins I due to spins S . The criterion for such an averaging is that $\omega_2 = \gamma_I H_2$ ($2H_2$ is the stirring field amplitude) be large compared to the rms second moment contribution to the nonresonant spins from either the resonant spins or the nonresonant spins whichever is greater. The

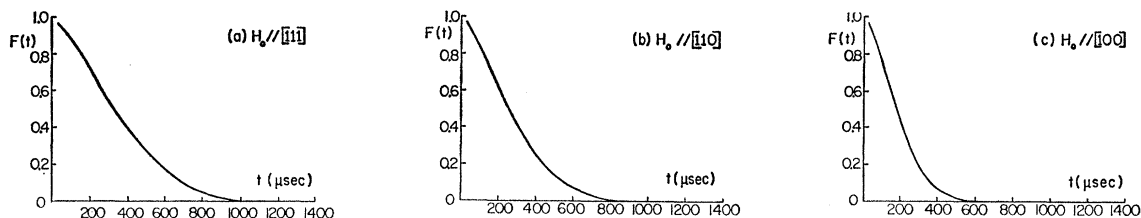
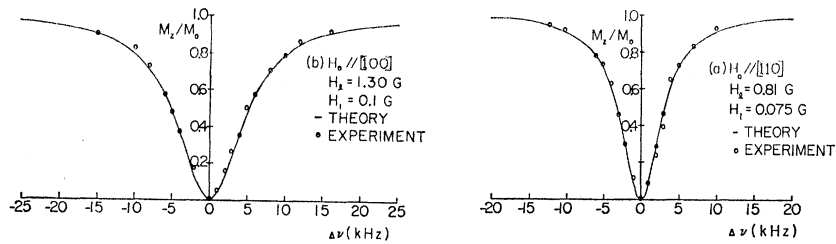


FIG. 3. Experimental free induction decays for the Cs^{133} nuclear-spin system in CsF.

⁸ L. R. Sarles and R. M. Cotts, Phys. Rev. **111**, 841 (1958).

FIG. 4. Relative magnetization as a function of $\Delta\nu$ for the F^{19} nuclear-spin system in CsF.



results are noted by observing the fid of spins **I** while spins **S** are being irradiated. In this experiment the second transmitter produced continuous rf at the F^{19} resonant frequency and the Cs^{133} fid was observed with H_0 parallel to a $\langle 100 \rangle$ crystal axis. The Cs^{133} resonance was set at 5.63868 MHz and the F^{19} line was irradiated at 40.4425 MHz. The strength of H_2 , the irradiating field, was varied from 0 to 16 G.

TABLE I. Measured T_1 values of F^{19} and Cs^{133} in two samples of CsF.

Nuclear species	Field orientation	Temperature ($^{\circ}K$)	Sample		
			F_0 (MHz)	T_1 (sec)	
Cs	[110]	77	6	700	B
Cs	[100]	77	6	723	B
F	[110]	77	19	70	B
F	[100]	77	19	77	B
Cs	[110]	293	6	480	A
Cs	[111]	293	6	400	A
Cs	[100]	293	6	510	A
F	[110]	77	11	17	A
F	[111]	77	11	14	A
F	[100]	77	11	22	A
F	[110]	293	11	50	A
F	[111]	293	11	50	A
F	[100]	293	11	50	A
Cs	[110]	77	6	350	A
Cs	[111]	77	6	350	A
Cs	[100]	77	6	430	A

Two CsF single crystals were used in the experiments. These were supplied by Semi-Elements, Inc. Both were cylinders $\frac{1}{2}$ in. long by $\frac{3}{8}$ in. diam. Sample A was cut with a $\langle 110 \rangle$ axis parallel to the cylinder axis, and sample B had its cylinder axis parallel to a $\langle 100 \rangle$ axis of the crystal.

In order to produce greater magnetization and therefore larger signals, low-temperature techniques

were used. The experiments were done with the sample immersed in a bath of liquid nitrogen maintained at the boiling point under atmospheric pressure. The nitrogen was contained in a glass Dewar flask.

RESULTS

Experimental fid curves for F^{19} and Cs^{133} resonance in CsF are shown in Figs. 2 and 3. Data are given for each species with H_0 parallel to the $[111]$, $[110]$, and $[100]$ axes of the crystal. Normalization of the curves to unity at $t=0$ is approximate since the initial amplitude is uncertain because of receiver dead time. Zero of the time scale is placed at the center of the rf pulse. Both samples A and B were studied. No difference could be noticed in the curves obtained from the two samples.

Results of the experiments to measure the local fields are shown in Figs. 4 and 5. Experimental points are direct measurements of M_z/M_0 as a function of $\Delta\nu$. Values of H_1 used in plotting the theoretical curves are those calculated from Eq. (9) considering only dipolar interactions. The time intervals τ_a and τ_b were equal in any one experiment and were 10 msec for studying F^{19} resonance, and 100 msec while studying Cs^{133} resonance.

Spin-lattice relaxation times for the two samples as determined experimentally are shown in Table I. These results are given to justify assumptions made about the relative lengths of T_1 , τ_a , and τ_b . The accuracy of the T_1 measurements is judged to be $\pm 10\%$ at $77^{\circ}K$ on the basis of scatter in the data.

Plots of initial cross-coupling transient slope as a function of pulse interval are given in Figs. 6 and 7. The initial fid amplitude is normalized to 10 V for plotting these data.

Figure 8 shows the Cs^{133} fid with H_0 parallel to the $[100]$ crystal axis obtained while irradiating the F^{19} resonance. Values of H_2 used are shown in the figure

FIG. 5. Relative magnetization as a function of $\Delta\nu$ for the Cs^{133} nuclear-spin system in CsF.

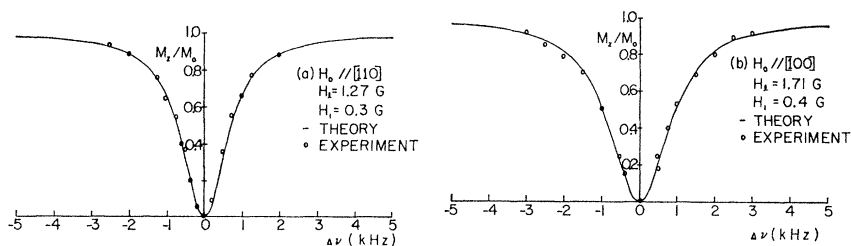


TABLE II. Theoretical and experimental second moments of F¹⁹ and Cs¹³³ resonances in CsF. All units are 10⁶ (rad/sec)².

	Field direction	$\langle \Delta\omega_F^2 \rangle_{F-F}$	$\langle \Delta\omega_F^2 \rangle_{F-Cs}$	$\langle \Delta\omega_F^2 \rangle_{Total}$	$\langle \Delta\omega_{Cs^2} \rangle_{Cs-Cs}$	$\langle \Delta\omega_{Cs^2} \rangle_{Cs-F}$	$\langle \Delta\omega_{Cs^2} \rangle_{Total}$
Dipolar theory	[100]	385	750	1135	3.04	35.8	38.8
	[110]	537	215	752	4.24	10.2	14.4
	[111]	595	42	637	4.78	2.0	6.8
Experiment	[100]			1090			45.0
	[110]			730			23.0
	[111]			640			13.1

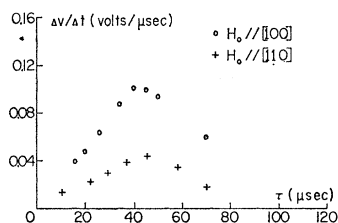
DISCUSSION OF RESULTS

The second and fourth moments of the absorption lines of F¹⁹ and Cs¹³³ resonances in CsF can be calculated using the formulae derived by Van Vleck.⁹ Appropriate lattice sums have been done by Ware¹⁰ to include 179 neighbors. Results of the calculations done considering only dipolar interactions are shown in Tables II and III.

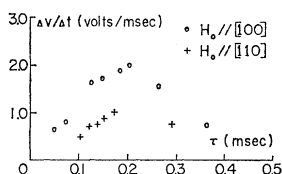
The fid function can be expressed as a series expansion

$$F(t) = \sum_{n=0}^{\infty} (-1)^n \frac{M_{2n}}{2n!} t^{2n}, \quad (10)$$

where M_n is the n th moment of the corresponding line shape. An estimate of the second moment can be ex-

FIG. 6. Initial slope of the observed cross-coupling transients as a function of pulse interval t for F¹⁹ resonance in CsF.

tracted from the experimental fid by plotting the experimental curve against t^2 for short times. If this program is extended to include the third term in the sum, an estimate of the fourth moment can also be made. Second and fourth moments have been extracted from the experimental F¹⁹ fid curves in this way, and the results are given in Tables II and III. Experimental

FIG. 7. Initial slope of the observed cross-coupling transients as a function of pulse interval t for Cs¹³³ resonance in CsF.⁹ J. H. Van Vleck, Phys. Rev. **74**, 1168 (1948).¹⁰ D. Ware, University of Nottingham, Nottingham, England (private correspondence).

F¹⁹ second and fourth moments are seen to be in agreement with those predicted from dipolar theory. Figure 9 shows a plot of $F_4(t) = 1 - \frac{1}{2}M_2t^2 + (1/4!)M_4t^4$ found from dipolar theory compared to the experimental curves.

It was noted that the experimental Cs¹³³ fid curves gave moments larger than those found from dipolar theory. In order to obtain an accurate value for the moments from the experiment, it was decided to fit a function proposed by Anderson¹¹ to the experimental curves. This function was introduced as a mathematical model of exchange narrowing, and it was chosen here because of its qualitative similarity to the experimental Cs¹³³ fid. The function is

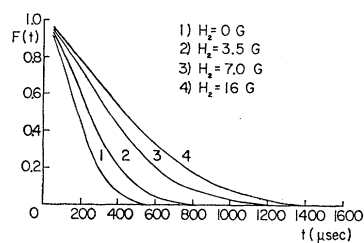
$$\phi(t) = \exp \left\{ -\frac{\omega_p^2}{\omega_e} t \int_0^{\omega_e t} \exp \left(-\frac{\pi}{4} x^2 \right) dx + \frac{2\omega_p^2}{\pi\omega_e^2} \left[1 - \exp \left(-\frac{\pi}{4} \omega_e^2 t^2 \right) \right] \right\}. \quad (11)$$

The corresponding second and fourth moments are

$$\langle \Delta\omega^2 \rangle = \omega_p^2, \quad (12)$$

$$\langle \Delta\omega^4 \rangle = 3\omega_p^2 + \pi/2\omega_p^2\omega_e^2. \quad (13)$$

Values of ω_p and ω_e are chosen to provide a good fit of $\phi(t)$ to the experiment. Plots of the resulting curves are shown in Fig. 10. The second and fourth moments thus found are given in Tables II and III as experimental findings. These are seen to be in excess of those predicted from dipolar theory.

FIG. 8. Experimental free induction decays for the Cs¹³³ nuclear spins in CsF obtained while irradiating the F¹⁹ resonance with a strong rf field. H_2 is the strength of the rf stirring field.¹¹ P. W. Anderson, J. Phys. Soc. Japan, **9**, 316 (1954).

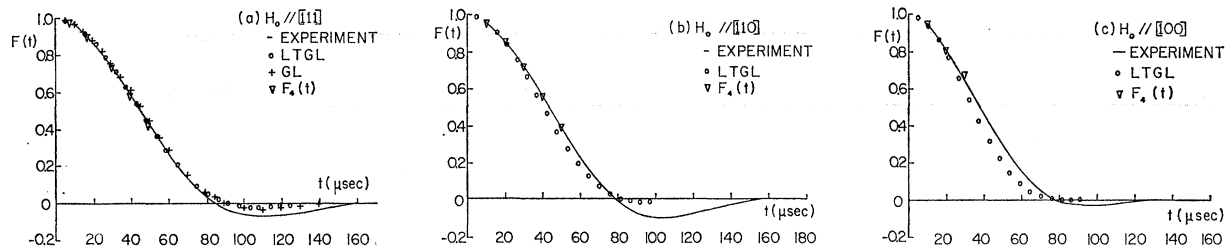


FIG. 9. Comparison of experimental and theoretical free induction decays for the F^{19} nuclear spins in CsF.

For F^{19} resonance at the $[111]$ orientation, the calculated second moment contributions indicate that the line broadening is due almost entirely to F-F interactions. The F^{19} spin system is expected to behave much like a single species system in this case. Figure 9(a) compares F^{19} experimental fid with H_0 parallel to a $\langle 111 \rangle$ crystal axis to the GL dipolar calculation for spin- $\frac{1}{2}$ systems in face-centered cubic crystals. The theoretical points agree closely with experiment, except in the late part of the curve.

The LTGL theory should be applicable to each fid studied. Their expression has been evaluated for CsF considering only dipolar interactions. The computations were done to include 728 neighbors. Results are compared to the experimental curves in Figs. 9 and 10. For F^{19} resonance there is fair agreement, the departure being more pronounced at the $[100]$ orientation, where the F-Cs interaction is strongest.

The Cs^{133} fid curves are not in agreement with LTGL dipolar theory. This, along with the moments shown in Tables II and III, indicates that interactions other than dipolar play a significant role in the Cs^{133} line broadening.

An interaction in addition to dipolar which significantly influences the Cs^{133} line shape would be expected to show in the local field measurements. However, results of these measurements are in substantial agreement with dipolar theory as shown in Fig. 5. The resolution of the local field experiments can be determined by finding the minimum value of H_1 above the saturation level, which affects the experimental curve. On this basis, it is concluded that measurements of H_1^2 are accurate to within 20% which corresponds to 10% accuracy for H_1 as shown in Table IV.

That dipolar theory is inadequate to describe the Cs^{133} resonance is seen also in the Cs^{133} fid curves ob-

tained while stirring the F^{19} spins with an rf field. On the basis of previous experimental work,⁸ it is expected that the contribution of the unlike spins to the second moment of the observed line would be eliminated by use of stirring fields of the strength employed. It was noted that no further change occurred in the Cs^{133} fid when the stirring field strength H_2 was increased from 10 to 16 G. If the cross-coupling contribution is eliminated, dipolar theory predicts the remaining second moment to be 3×10^6 (rad/sec)². But the observed second moment does not fall below about 14×10^6 (rad/sec)² when the rf stirring is applied, indicating the presence of some broadening mechanism other than dipolar.

The above results could be understood qualitatively on the basis of an interaction which appreciably affects the Cs^{133} line shape but not that of F^{19} . This interaction must contribute to the Cs^{133} second moment without being observable in the local-field measurements. Scalar exchange does not satisfy these conditions since it contributes to the local field but not to the second moment.

Since Cs^{133} nuclei possess electric quadrupole moments, quadrupole effects could play a role in the experimental findings. This would be consistent with the first qualitative feature assigned to the additional mechanism since the F^{19} nuclei have spin $\frac{1}{2}$.

The quadrupole contribution to the second moment can be calculated using the same assumption employed to calculate the quadrupole contribution to the local field. This gives the result

$$\gamma I^2 H_{1q}^2 / \langle \Delta \omega_I^2 \rangle_Q = \frac{1}{3}. \quad (14)$$

If the differences between the dipolar second moments and the experimental values are attributed to quadrupole effects, the corresponding contribution to the local

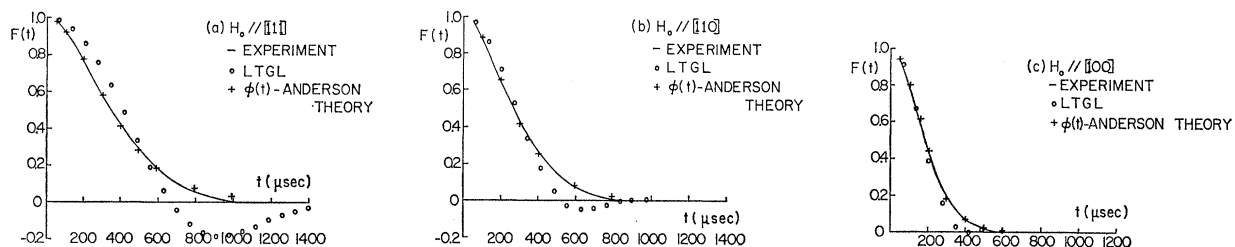


FIG. 10. Comparison of experimental and theoretical free induction decays for the Cs^{133} spins in CsF.

TABLE III. Theoretical and experimental fourth moments of F^{19} and Cs^{133} resonances in CsF. All units are 10^{15} (rad/sec)⁴.

	Field direction	$\langle \Delta\omega_{F^4} \rangle_{F-F}$	$\langle \Delta\omega_{F^4} \rangle_{F-Cs}$	$\langle \Delta\omega_{F^4} \rangle_{Total}$	$\langle \Delta\omega_{Cs^4} \rangle_{Cs-Cs}$	$\langle \Delta\omega_{Cs^4} \rangle_{Cs-F}$	$\langle \Delta\omega_{Cs^4} \rangle_{Total}$
Dipolar theory	[100]	375	5000	5380	0.0218	6.63	6.64
	[110]	640	810	1450	0.0387	1.65	1.70
	[111]	872	110	980	0.0504	0.22	0.27
Experiment	[100]			5040			7.20
	[110]			1500			2.18
	[111]			1010			0.70

TABLE IV. Theoretical and experimental values of H_i in CsF.

	Nuclear species	H_2 (G)	
		$H_{0 [100]}$	$H_{0 [110]}$
Dipolar Theory	F^{19}	1.30	0.81
	Cs^{133}	1.71	1.27
Experiment	F^{19}	1.3 ± 0.13	0.8 ± 0.1
	Cs^{133}	1.7 ± 0.17	1.3 ± 0.13

field can be found using (14). At the [100] and [110] orientations, H_{i0} is thus found to be 0.17 and 0.23 G, respectively. It is noted that these values are within the 10% margin of resolution ascribed to the local-field measured values.

Initial cct slopes as shown in Figs. 6 and 7 agree only qualitatively with dipolar theory. Since these experiments are directly concerned with the Cs-F interactions, the fact that dipolar theory does not account for the Cs^{133} line shape could explain this discrepancy. It was observed that these measurements are affected by the size of the transmitter coil and thus the inhomogeneity of the rf field.

CONCLUSIONS

The GL theory satisfactorily describes free induction decays in spin systems for cases which closely resemble the single-ingredient situation and the spins are coupled by dipolar interactions. LTGL theory adequately predicts the fid in two species samples where only dipolar interactions need be considered.

Some interaction other than dipolar must be included to account for the experimental Cs^{133} fid curves in CsF. Qualitative features of the experimental results indicate this to be coupling of the Cs^{133} nuclear electric quadrupole moments with electric field gradients in the crystal.

The local fields in crystalline CsF are in substantial agreement with dipolar theory. Results of the present work indicate, however, that local-field measurements of the type described here are relatively insensitive to quadrupole effects.

The cct measurement technique of Mansfield may lead to erroneous conclusions if the rf field is not sufficiently homogeneous over the sample volume. However, no theoretical explanation for this seems to be apparent.